

# Investigations of aerosol formation pathways during MSW combustion based on high-temperature impactor measurements

Thomas Brunner<sup>1,2,3\*</sup>, Juergen Fluch<sup>1</sup>, Ingwald Obernberger<sup>1,2,3</sup>, Ragnar Warnecke<sup>4</sup>

<sup>1</sup> Bioenergy 2020+ GmbH, Inffeldgasse 21b, A-8010 Graz, Austria  
Tel.: +43 316 48130013; Fax: +43 316 4813004  
thomas.brunner@bioenergy2020.eu

<sup>2</sup> BIOS BIOENERGIESYSTEME GmbH, Inffeldgasse 21b, A-8010 Graz, Austria  
office@bios-bioenergy.at

<sup>3</sup> Institute for Process and Particle Engineering, Graz University of Technology  
Inffeldgasse 21b, A-8010 Graz, Austria  
ingwald.obernberger@tugraz.at

<sup>4</sup> Gemeinschaftskraftwerk Schweinfurt GmbH  
Hafenstraße 30, 97424 Schweinfurt, Germany  
ragnar.warnecke@gks-sw.de

\* corresponding author

## ABSTRACT

In order to gain deeper insights into aerosol formation processes during MSW combustion, test runs with a specially developed high-temperature aerosol measurement and sampling device, the so called high-temperature impactor (HTI), as well as subsequent chemical analyses of the particles sampled have been performed at a real-scale plant. The results show that aerosol formation during MSW combustion is based on the volatilisation of minor amounts of Si-, Ca-, Mg- and Al-compounds followed by nucleation in the fuel bed region which is then followed by excessive condensation of alkaline metal sulphates and especially chlorides in the radiative and the convective boiler sections. At lower flue gas temperatures in the superheater as well as the economiser section also the condensation of heavy metal (Zn, Pb) chlorides provides contributions to aerosol formation.

**Keywords:** MSW combustion, aerosols, high-temperature sampling

## 1. INTRODUCTION AND OBJECTIVES

Ash related problems such as deposit formation, corrosion and particulate emissions are of great relevance when utilising ash rich fuels like municipal solid waste (MSW), waste wood, straw and other agricultural biomass fuels in combustion plants. Consequently, investigations focusing on the characterisation and formation of fly ashes, especially of aerosols, are of basic interest for the conception, design and operation of such plants. In general, fly ashes formed during the combustion of solid fuels can be divided into coarse fly ashes and aerosols (particles <1 µm). In grate-fired combustion plants coarse

fly ashes result from the entrainment of small ash, fuel as well as char particles from the fuel bed with the flue gases. The size of these particles usually is in the range between some  $\mu\text{m}$  and some  $100 \mu\text{m}$ . They are partly precipitated in the furnace and the boiler (so called furnace and boiler ashes) by gravitational and centrifugal forces or form boiler and superheater deposits. The remaining particles leave the boiler as coarse fly ash emission. Coarse fly ashes typically consist of refractory species such as Ca, Si, Mg, Fe, Al, K and P, and additionally contain compounds of semivolatile (K, Na) and easily volatile (S, Cl, easily volatile heavy metals) elements which condense on the surfaces of the coarse fly ashes or undergo surface reactions.

Aerosols (fine particulate matter with a particle size  $<1 \mu\text{m}$ ) on the other side mainly consist of semivolatile and easily volatile elements such as K, Na, Zn, Pb, S and Cl. During combustion of P-rich fuels also P may considerably contribute to aerosol formation. The formation mechanisms involved are significantly more complex than those responsible for coarse fly ash formation. During combustion volatile inorganic compounds are partly released from the fuel to the gas phase. The most relevant elements involved are K, Na, S and Cl as well as easily volatile heavy metals (e.g.: Zn, Pb). Subsequently they undergo gas phase reactions. If one of the compounds formed becomes supersaturated, gas to particle conversion takes place. This supersaturation can thereby result from the excessive formation of a distinct compound as well as from the formation of reaction products which have a lower saturation vapour pressure than the reactants. Additionally, the cooling of the flue gases in the radiative and the convective boiler sections leads to supersaturation due to the decrease of the saturation vapour pressures with decreasing flue gas temperatures. For gas to particle conversion nucleation (the formation of new particles) as well as condensation on already existing particles and heat exchanger surfaces are the mechanisms concerned. Since with decreasing particle size the specific surface area of a particle significantly increases, ash forming vapours preferably condense on small particles (aerosols) and to a less extent on coarse fly ashes.

Besides the already addressed semivolatile and easily volatile elements also smaller concentrations of refractory species such as Si, Ca, Mg and Al are usually found in the aerosol fraction. For these elements two different aerosol formation pathways are known. The first one concerns mineral grains (impurities) included in the fuel which are partly fragmented during the rapid heating of the fuel during combustion by thermal stress and thereby form particles in the size range from below  $1 \mu\text{m}$  to some  $\mu\text{m}$  [1]. Second, at high temperatures and reducing atmospheres, as they prevail in char particles during burnout, Si, Mg and Ca-oxides embedded in the fuel matrix may be reduced to easily volatile suboxides (e.g. SiO or  $\text{Al}_2\text{O}$ ) or metals which are released to the gas phase. As soon as they enter zones with decreasing temperatures and increasing oxygen partial pressure they form oxides which due to their low saturation vapour pressures nucleate to particles in the size range of some nm [1, 2].

The already mentioned condensation of ash forming vapours on aerosol surfaces as well as coagulation of aerosol particles in the furnace and the boiler lead to particle growth which finally results in the typical particle size distribution of aerosols at boiler outlet characterised by one distinct peak in the range  $<1 \mu\text{m}$ . With increasing release of aerosol forming elements from the fuel to the gas phase and consequently with increasing mass of aerosol particles formed, the average particle diameter as well as the peak diameter of

the aerosol particle size distribution increase due to enforced surface condensation and agglomeration.

The detailed understanding of the mechanisms and processes briefly introduced above is not only essential for the description of particle formation during combustion, it also provides basic information regarding the constraints for deposit formation processes in the radiative and the convective boiler sections as well as the simulation of these processes. Therefore, already in the 1990ies simulation routines regarding aerosol formation during combustion processes have been developed [3, 4, 5]. However, so far experimental methods applicable for the validation of the simulation results regarding the high temperature sections of real-scale combustion plants (furnace, boiler) did not exist. Therefore, within the EU-funded research project BIOASH (EU FP6 Project SES-CT-2003-502679) an unique device for the determination of the particle size distribution and concentration of aerosols in flue gases at temperatures of up to 1,000°C has been developed at the Institute for Process and Particle Engineering, Graz University of Technology. The particles sampled with this device can also be subsequently analysed by means of wet chemical analyses as well as SEM/EDX [6]. This so called high-temperature impactor (HTI) has already been successfully applied within studies regarding aerosol formation in real-scale biomass combustion processes (wood, waste wood and straw combustion) as well as in biomass co-firing in coal-fired power plants [7]. Within the work presented in this paper, the HTI was for the first time applied in order to investigate aerosol formation in a real-scale MSW combustion plant.

The aim of the work was to perform HTI sampling and measurements at 4 different measurement positions of one line of the MSW incineration plant at GKS GmbH in Schweinfurt, Germany. Thereby, the concentrations of particles <1 µm in the flue gas, their particle size distributions and their chemical compositions should be determined in order to study and discuss aerosol formation processes during MSW combustion.

## 2. Materials and methods

### 2.1 Plant description and measurement positions

Test runs have been performed at line 2 of the MSW combustion plant at GKS GmbH in Schweinfurt, Germany. The plant consists of 3 identical lines with a grate-fired combustion unit with a 4-path boiler (steam parameters: 25 t/h at 65 bar and 435°C) with 20.8 MW<sub>NCV</sub> nominal fuel power each. Multi-cyclones, a baghouse filter as well as a 2-stage scrubber are applied for flue gas cleaning.

The measurement positions were chosen at 4 positions along the way of the flue gas through the boiler in order to investigate the influence of the temperature profile along the flue gas flow on aerosol formation (see Figure 1). Measurement position 1 (Pos.1) was located in the 1<sup>st</sup> duct about 9 m above the secondary air injection. The flue gas temperature at this position is about 1,000°C. Measurement position 2 (Pos.2) was in the lower part of the 2<sup>nd</sup> duct (flue gas temperatures of about 670°C). The measurement positions 3 and 4 were located in the middle of the superheater section (Pos.3 at about 550°C) respectively downstream the first economiser (Pos.4 at about 360°C).

During three subsequent test run days at least one measurement per position has been performed. Prior to the measurements, the flue gas temperatures at Pos.1, Pos.2 and Pos.3

have been checked with a suction pyrometer. For the evaluation of the test runs the readings of the plant internal thermocouples located next to the measurement positions have been corrected with the results of these pyrometer measurements (see also Figure 1).

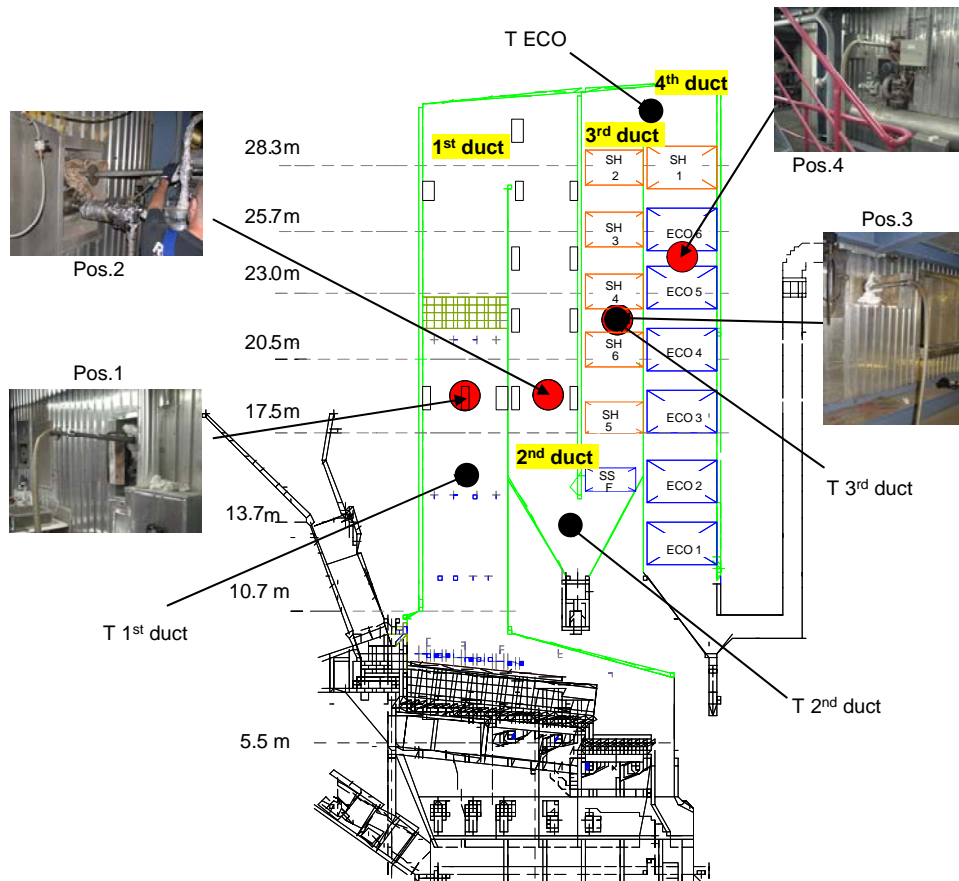


**Figure 1:** Scheme of the combustion plant as well as measurement positions  
 Explanations: Pos.1 , 2, 3, 4: measurement positions; T ... positions of the plant internal temperature measurements next to the sampling positions; SH ... superheater; ECO ... economiser

## 2.2 High-temperature impactor (HTI)

The development of the high-temperature low-pressure impactor (HTI) is based on the common design of a Berner-type low-pressure impactor (BLPI). Flue gas is sucked through the impactor and is forced to change flow direction for several times. This is realized by a number of subsequent impaction stages each consisting of an orifice plate, a spacer ring and a stagnation plate (see Figure 2). Particles which are too large to follow the changing flow directions between the orifice plate and the stagnation plate are precipitated on a sampling foil placed on the stagnation plate. The cut diameter of each stage is defined by the volumetric flow rate through the impactor, the number and diameter of identical orifices and the distance between the orifice plate and the stagnation plate. Moreover, the cut diameter is also a function of the flue gas temperature. In the sequence of the stages the number and diameter of the orifices as well as the distance between the orifice plate and the stagnation plate are changed stage by stage in a way that

the cut diameters of the stages decrease. The cut diameters of the impactor stages for different temperatures are presented in Figure 3.

The HTI consists of 8 stages. A critical orifice downstream of the last impactation stage controls flue gas flow through the impactor. The impactor is covered with an inner casing where it is fixed by a strong spring in order to avoid leakages. The inner casing is then inserted into an outer casing which is finally placed in the flue gas flow. The single parts of the HTI are manufactured from different heat resistant alloys. Due to thermal and chemical stability Pt-foils have been chosen as sampling media.



**Figure 2:** Scheme of the high-temperature impactor (HTI) (left) as well as HTI directly after a measurement (right)

Explanations: 1 ... outer casing, 2 ... inner casing, 3 ... shell, 4 ... orifice plate, 5 ... spacer ring, 6 ... stagnation plate, 7 ... critical orifice, 8 ... spring

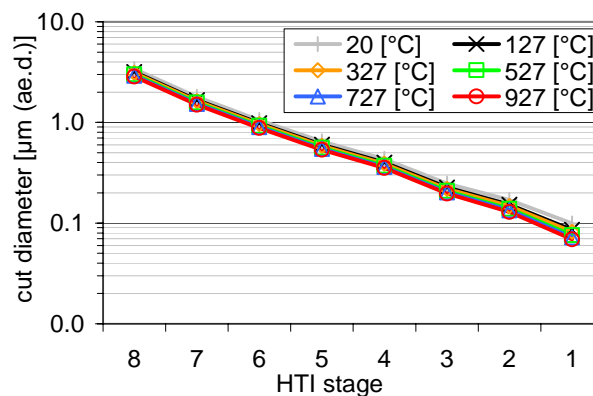


**Figure 3:** Cut diameters of the HTI stages as a function of temperature

Explanations: ae.d. ... aerodynamic diameter

Prior to sampling the HTI is positioned in the measurement position for 20 to 30 minutes for pre-heating. Pre-heating is needed to avoid cooling of the flue gas and particle formation by nucleation as well as ash vapour condensation in the HTI [6]. The sampling time (time during which flue gas is sucked through the HTI) itself is restricted to some minutes in order to avoid particle overloading. The Pt foils are weighed prior and after the sampling and based on the weight gain and the flue gas flow through the HTI during the sampling period the particle concentration for each stage is calculated (in mg/Nm<sup>3</sup>).

## 2.3 Chemical and SEM/EDX analyses of aerosols

To gain detailed information concerning aerosol formation processes the chemical compositions of particle samples taken with the HTI at the different measurement positions have been determined by wet chemical analyses as well as SEM/EDX (Scanning Electron Microscopy / Energy Dispersive X-ray Spectrometry). From former studies it is well known that the masses and compositions of the depositions found below each orifice on the sampling foils do not significantly vary within one sampling foil. Consequently, it is possible to cut the foils into different sectors and analyse the different sectors with different methods, i.e. electron microscopy and wet chemical analyses.

Accordingly, the sampling foils 1 to 6 of selected HTI measurements have been prepared for analyses. It has to be mentioned, that the major analyses work has been performed by SEM/EDX while wet chemical analyses have only been applied in order to check the results of the SEM/EDX measurements and to make sure, that the zones of the particle depositions which have been analysed are representative for the whole sample. For wet chemical analyses the particles were washed from the foils and digested with either deionised water (for Cl-analyses) or for all other elements with a mixture of HNO<sub>3</sub> (65%) / HF/ H<sub>3</sub>BO<sub>3</sub>. Cl detection was performed by ion chromatography and Al, Ca, Cd, Cu, Fe, K, Mg, Mn, Na, P, Pb, S, Si und Zn detection by ICP-OES or ICP-MS (depending on the concentration level). For SEM/EDX analyses the samples were coated with carbon. In this paper the results of the wet chemical analyses are not presented since they have been in good agreement with the results of the SEM/EDX analyses which are discussed in detail in the following sections.

## 3. Results

### 3.1 Concentrations and particle size distributions of aerosols

In Table 1 and Figure 4 the results of the HTI measurements at the 4 sampling positions are summarised. Additionally, in Figure 5 the average particle size distributions of the aerosol fractions (mean values of 3 measurements) are presented. The flue gas temperatures mentioned represent data taken from the plant internal temperature measurements (see Figure 1) which have been corrected with the results of the pyrometer measurements performed prior to the test runs (see section 2.1).

At Pos.1 (1<sup>st</sup> duct) a distribution maximum in the particle size range <1 µm can be identified between the 3<sup>rd</sup> and the 4<sup>th</sup> HTI stage (cut diameter: 0.18 µm respectively 0.33 µm). This peak results from particle formation by nucleation and subsequent coagulation of particles. Compounds with comparably low saturation vapour pressures which undergo gas to particle conversion at high temperatures directly above the fuel bed are assumed to be the constituents of these particles (see also section 3.2). Moreover, a slight increase of the particle concentrations in the size range >1 µm can be identified which may be due to particles which originate from the thermal fragmentation of minerals. The particle concentration of the HTI stages 1 to 5 (particles <0.84 µm) amounts to 281 to 568 mg/Nm<sup>3</sup> (related to dry flue gas and 11 vol% O<sub>2</sub>).

At Pos.2 a distinct peak on the 5<sup>th</sup> HTI stage (cut diameter: 0.58 µm), as well as a local maximum on the 2<sup>nd</sup> HTI stage (cut diameter: 0.13 µm) are found. The local maximum

represents a typical nucleation peak and results from particle formation due to a high supersaturation of a distinct compound in the region between Pos.1 and Pos.2. At the measurement positions downstream Pos.2 this local maximum disappears again due to particle growth by condensation and coagulation. The average aerosol concentration (HTI stages 1 to 5 respectively particles  $<0.91 \mu\text{m}$ ) at Pos.2 amounts to 1,214  $\text{mg}/\text{Nm}^3$ .

**Table 1:** Average aerosol concentrations at the 4 measurement positions

Explanations: flue gas temperatures: average temperatures at the measurement position during the HTI measurement; measurement positions: see Figure 1

| Measurement position  |                       | Pos.1 | Pos.2   | Pos.3   | Pos.4   |
|---|-----------------------|-------|---------|---------|---------|
| Number of single measurements   | [-]                   | 3     | 3       | 3       | 3       |
| Average flue gas temperature  | [°C]                  | 978.4 | 673.5   | 541.4   | 363.0   |
| Average aerosol concentration (dry flue gas; 11 vol% O <sub>2</sub> ) | [mg/Nm <sup>3</sup> ] | 384.1 | 1,214.4 | 1,753.8 | 1,181.1 |

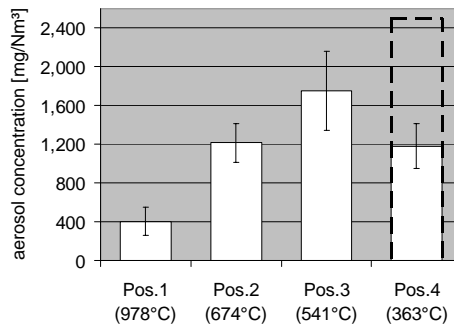


**Figure 4:** Average aerosol concentrations at the 4 measurement positions

Explanations: total of the HTI stages 1 to 5; all data related to dry flue gas and 11 vol% O<sub>2</sub>; mean values and standard deviations from 3 single measurements; dashed line: particle concentration at Pos.4 calculated from the results of the chemical analyses

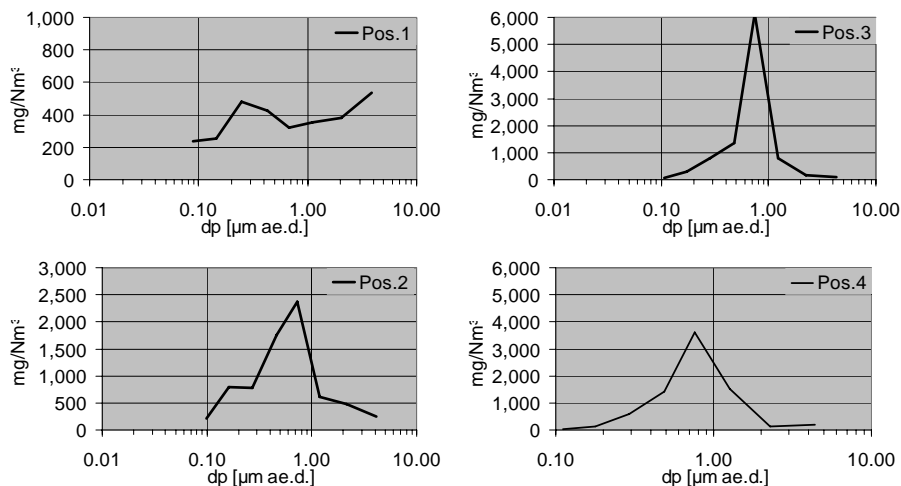


**Figure 5:** Particle size distributions of the aerosol fraction

Explanations: all data related to dry flue gas and 11 vol% O<sub>2</sub>; mean values from 3 single measurements; ae.d. ... aerodynamic diameter

At Pos.3 a distinct distribution peak can be found on the 5<sup>th</sup> HTI stage (cut diameter: 0.59  $\mu\text{m}$ ), the average aerosol concentration amounts to 1,754  $\text{mg}/\text{Nm}^3$  (particles  $<0.94 \mu\text{m}$ ). Also in the 4<sup>th</sup> duct the peak diameter of the aerosol particle size distribution is located on the 5<sup>th</sup> HTI stage (cut diameter: 0.60  $\mu\text{m}$ ). The average aerosol concentration (particles  $<0.96 \mu\text{m}$ ) amounts to 1,181  $\text{mg}/\text{Nm}^3$  and therefore is lower than the one determined at Pos.3. This is a surprising result which, due to the high decrease of the particle concentration cannot be explained with deposit formation on heat exchanger tubes between the two measurement positions. It is assumed that at the measurement position purge air strains from the soot blowers could have caused a dilution of the flue gas and might have been responsible for the lower particle concentrations. However, from the results of the chemical analyses performed with the samples taken at Pos.3 and Pos.4 it can be deduced that the particle concentration in the flue gas at Pos.4 should amount to about 2,500  $\text{mg}/\text{Nm}^3$  (see also section 3.2).

When analysing the trend of the particle size distribution peaks over the 4 measurement positions, a clear particle growth between Pos.1 and Pos.2 can be recognised. A less pronounced particle growth effect is seen between Pos.2 and Pos.3. The particle growth between Pos.1 and Pos.2 is besides agglomeration mainly related to the high amount of surface condensation of aerosol forming matter (the aerosol concentration increases from in average 384 to in average 1,214  $\text{mg}/\text{Nm}^3$ ). Between Pos.2 and Pos.3 gas to particle conversion rates decrease (the average particle concentration increases from 1,214 to 1,754  $\text{mg}/\text{Nm}^3$ ) and consequently also particle growth is less pronounced. According to the analyses data presented in section 3.2, about the same should also be true for the section between Pos.3 and Pos.4, however, the effect cannot be proven based on the gravimetric evaluation of the HTI measurements due to the already mentioned reasons.

### 3.2 Chemical compositions of the aerosol samples

In Figure 6 the results of the SEM/EDX analyses of the stages 1 to 6 of selected HTI measurements performed at the 4 measurement positions are summarised.

At Pos.1 all size classes investigated show rather high concentrations of Ca and Si. As already mentioned, the high temperatures and reducing atmosphere prevailing in char particles during burnout can lead to a reduction of refractory oxides to suboxides (e.g. SiO, Al<sub>2</sub>O) or elemental metals which are easily volatile and therefore can be released to the gas phase. After diffusion to the char surface they enter zones with higher oxygen partial pressures and therefore form oxides which, due to their low saturation vapour pressure, nucleate. In the following these particles grow by coagulation. In Figure 6 close-up SEM-images (stage 3) of particles consisting mainly of Si and lower amounts of Ca, K and Na, which may have formed according to the mechanism mentioned above are presented.

By this mechanism the high Si and Ca-concentrations as well as the somewhat lower Al and Mg-concentrations on the samples from stage 1 to 5 can be explained. Moreover, minor concentrations of Zn can be detected in the sample taken at Pos.1. Also Zn can be released under reducing conditions to the gas phase as elemental Zn. As soon as oxidising conditions prevail Zn forms ZnO and subsequently nucleates. This mechanism is already well known from waste wood combustion [7, 8]. With increasing particle size an increase

of the Ca and Mg-concentrations on stage 6 can be observed which is most probably due to the fragmentation of Ca and Mg-rich minerals.

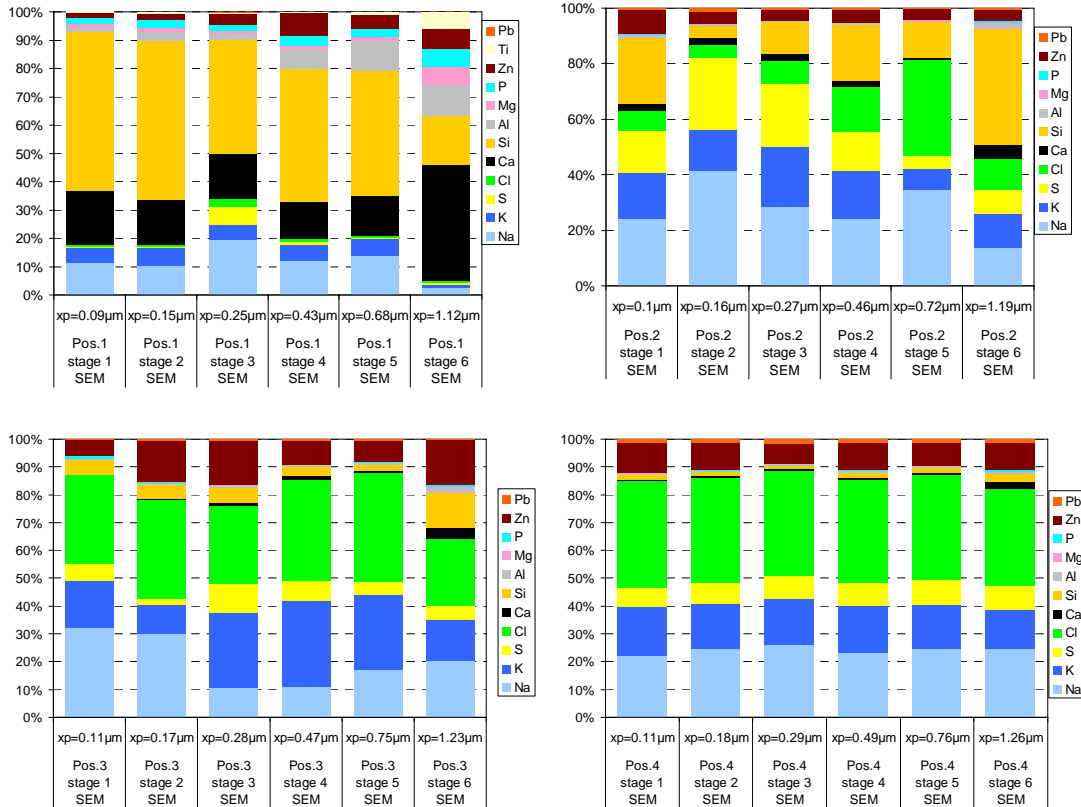


**Figure 6:** Results of the SEM/EDX analyses of the stages 1 to 6 of selected HTI measurements performed at the 4 measurement positions

Explanations: concentration in atom% not considering oxygen; xp ... geometric mean diameter of the respective impactor stage (aerodynamic diameter)

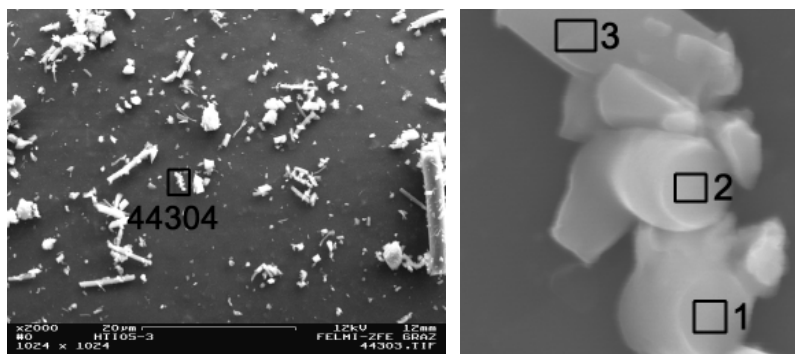


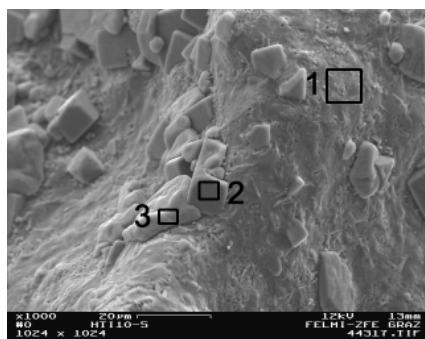
**Figure 7:** SEM-image of an area on stage 3 of a HTI sample taken at Pos.1

Explanations: left image: overview; right image: close-up of area 44304; picture width: 1.5µm; results of the EDX-analyses of the numbered areas (atom%): area 1: Si: 21.2%, Ca: 4.9%, Na: 1.9% rest: O; area 2: Si: 26.3%, Ca: 2.2%, Na: 2.8% rest: O; area 3: Si: 29.0%, Na: 2.9% K: 1.2% rest: O

Particle formation by the condensation of easily volatile ash forming compounds only provides minor contributions to particle formation in the section before Pos.1. The analyses results presented in Figure 6 show elevated Na and S concentrations on stage 3 of the HTI indicating that gas to particle conversion of Na<sub>2</sub>SO<sub>4</sub> has already been initialised. This is not surprising since, when taking the whole amount of Na<sub>2</sub>SO<sub>4</sub> which condenses into consideration, Na<sub>2</sub>SO<sub>4</sub> saturation is already reached at temperatures between 1,100 and 1,200°C. Besides stage 3 also on the other HTI stages considerable K and Na concentrations are detected, however, due to the fact that no S is present, Na and K seem to be embedded in the Si-rich structures as confirmed by the EDX analyses presented in Figure 7.

As the results of the SEM/EDX analyses (Figure 6) clearly show, particles sampled at Pos.2 mainly consist of Ca, Si, Mg, Al, K, Na, Zn, S and Cl. In comparison with the sample from Pos.1 the concentrations of refractory species (Ca, Si, Mg, Al) significantly decrease while the concentrations of easily volatile and semivolatile elements (K, Na, S, Cl, etc.) increase. During the cooling of the flue gas in the section between Pos.1 and Pos.2 supersaturation of alkaline metal sulphates and chlorides followed by nucleation and condensation takes place. Since the formation of Si, Ca, Mg and Al-rich particles has already been finalised close above the fuel bed, a “dilution” of these elements with condensing matter occurs which leads to the decreasing Ca and Si concentrations.

For particle formation and growth in the section between Pos.1 and Pos.2 the behaviour of alkaline metal sulphates and chlorides is of major interest. As already mentioned, Na<sub>2</sub>SO<sub>4</sub> starts to nucleate/condense at temperatures as high as 1,100°C. Due to rapid cooling of the flue gases high saturation ratios of Na<sub>2</sub>SO<sub>4</sub> occur which favour the nucleation process instead of condensation on surfaces and explain the high Na and S concentrations on stage 2 of the HTI sampled at Pos.2 (nucleation peak). The K<sub>2</sub>SO<sub>4</sub> vapour pressure is higher than the one of Na<sub>2</sub>SO<sub>4</sub> and consequently K<sub>2</sub>SO<sub>4</sub>-particle formation starts at slightly lower temperatures. Since K is quite evenly distributed over the HTI stages condensation is assumed to be the governing gas to particle conversion mechanism. The phase change of chlorides takes place at considerably lower temperatures (due to the higher vapour pressure of chlorides) however, at about 674°C at Pos.2 KCl and NaCl condensation has already been initiated. In Figure 8 a close-up of stage 3 of a HTI-sample taken at Pos.2 is presented. As the SEM/EDX analyses show, the deposition consists mainly of Na and K sulphates as well as spots with NaCl and KCl.



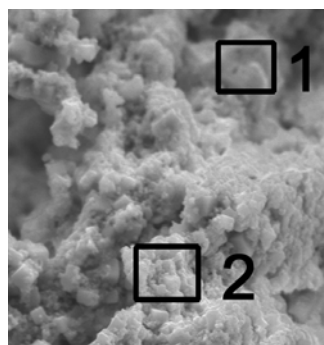
| Area            | 1    | 2    | 3    |
|-----------------|------|------|------|
| Si              | 1.7  |      |      |
| Ca              | 1.2  |      |      |
| Na              | 8.4  | 40.1 | 1.1  |
| K               | 15.3 |      | 46.6 |
| S               | 12.4 |      |      |
| Cl              | 3.0  | 51.2 | 45.7 |
| Zn              | 1.3  | 1.3  |      |
| rest (mainly O) | 56.8 | 7.3  | 6.6  |

**Figure 8:** SEM-image and EDX-analyses of stage 3 of a HTI sample taken at Pos.2  
 Explanations: data in atom%

Moreover, also the Zn-concentrations increase in comparison with the sample taken at Pos.1. From the element balances it can be deduced that Zn is most probably present as ZnCl<sub>2</sub>.

From Pos.2 to Pos.3 the Zn, K and Cl-concentrations further increase. Since the vapour pressure of KCl is higher than the one of NaCl, KCl condensation starts at slightly lower temperatures and is intensified in the boiler section between Pos.2 and Pos.3. As element balances considering thermodynamically plausible compounds show, the Na and K detected cannot bind all the S and Cl and therefore it can be assumed, that Zn is mainly present as ZnCl<sub>2</sub>. Moreover, minor concentration of Pb (most probably PbO according to the temperature range) are detected. As already mentioned for Pos.2, the enforced condensation of K and Na chlorides leads to a further dilution of the already existing particles and hence the Si, Ca, Al and Mg concentrations decrease compared to Pos.2.

Regarding Pos.4 the chemical composition over the different size ranges investigated is rather homogeneous which is mainly due to coagulation effects. The main constituents of the aerosols are K and Na-chlorides and to a minor extent K and Na-sulphates. Compared with Pos.3 the Zn-concentration increases due to condensation of most probably ZnCl<sub>2</sub> and also the Pb-concentrations significantly increase. As Figure 9 shows, Pb is present as PbCl<sub>2</sub> which seems also thermodynamically plausible regarding the temperature level at Pos. 4.



| Area            | 1    | 2    |
|-----------------|------|------|
| Si              |      | 2.5  |
| Na              | 3.6  | 27.8 |
| K               | 15.5 | 6.9  |
| S               |      | 5.0  |
| Cl              | 48.0 | 27.3 |
| Zn              | 2.9  | 3.4  |
| Pb              | 15.9 |      |
| rest (mainly O) | 9.6  | 25.2 |

**Figure 9:** SEM-image and EDX-analyses of stage 5 of a HTI sample taken at Pos.4  
 Explanations: data in atom%; picture width: 20 µm

As already mentioned in section 3.1, the gravimetric evaluation of the HTI-measurements performed at Pos.4 resulted in non-plausible aerosol concentrations. Assuming that in the section between Pos.1 and Pos.4 no additional Si, Ca, Mg and Al particle formation takes place (i.e. the mg/Nm<sup>3</sup> of these elements in the flue gas remain the same) and based on the analyses of the HTI samples taken at Pos.4, a concentration of aerosols in the flue gas of about 2,500 mg/Nm<sup>3</sup> (dry flue gas, 11 vol% O<sub>2</sub>) can be calculated for Pos. 4.

## 4. Summary and conclusions

The HTI-measurements showed an increase of the aerosol concentrations with decreasing flue gas temperatures from the 1<sup>st</sup> duct of the furnace (384 mg/Nm<sup>3</sup> related to dry flue gas and 11 vol% O<sub>2</sub>; flue gas temperature of in average 978°C) over the 2<sup>nd</sup> duct (1,214 mg/Nm<sup>3</sup> at 674°C) to the 3<sup>rd</sup> duct (1,754 mg/Nm<sup>3</sup> at 541°C). In the 4<sup>th</sup> duct however, a

decrease to 1,181 mg/Nm<sup>3</sup> (at 350°C) occurred according to the gravimetric evaluation of the measurements. This decrease is most probably due to influences of air strains from soot blower purge air. According to estimations based on the concentration trends of Si, Ca, Mg and Al in the aerosols at the different measurement positions, the aerosol concentration in the 4<sup>th</sup> duct should be in the range of 2,500 mg/Nm<sup>3</sup>.

Taking the trends of the aerosol concentrations in the flue gas at the different measurement positions as well as the chemical compositions of the particles into consideration, particle formation during MSW combustion can be described as follows. As a first step easily volatile and semivolatile elements such as K, Na, Zn, Pb as well as S and Cl are partly released from the fuel bed to the gas phase. At the same time mineral inclusions in the fuel are fragmented by thermal stress during the combustion of the fuel and thereby form particles in the size range of below 1 µm up to some µm which are entrained from the fuel bed. Moreover, Si, Ca, Mg and Al-compounds are reduced to suboxides or elemental metals at high temperatures and reducing atmosphere in the char and are also released. As soon as they reach regions with increasing oxygen partial pressure they form oxides and nucleate (form particles in the size range of some nm). When the flue gas temperatures start to decrease, nucleation of Na<sub>2</sub>SO<sub>4</sub> and K<sub>2</sub>SO<sub>4</sub> starts and as soon as a critical surface of the particles already formed is available condensation of alkaline metal sulphates, chlorides as well as heavy metal chlorides is the dominating process. According to their saturation vapour pressures with decreasing temperatures first Na<sub>2</sub>SO<sub>4</sub> and K<sub>2</sub>SO<sub>4</sub> start to condense followed by NaCl, KCl, ZnCl<sub>2</sub> and PbCl<sub>2</sub>. Condensation of ash forming vapours on already existing particle surfaces as well as coagulation processes thereby lead to the typical unimodal particle size distribution of the aerosol fraction which usually is determined at boiler outlet.

As the measurements and analyses show, condensation of Cl-containing compounds is already initialised before superheater inlet. These aerosol particles, which have already been formed provide only minor contributions to deposit formation since they follow the streamlines around the heat exchanger tubes. However, the most intensive condensation takes place in the superheater section and there condensation on particle surfaces is in competition with condensation on superheater surfaces. Consequently, a high potential for deposit formation by alkali metal and heavy metal chlorides exists. This is especially true for the superheater inlet where the flue gas is still comparably hot and a high temperature gradient between the flue gas and the tube surfaces exists. Especially with increasing deposit thickness and consequently increasing deposit surface temperatures, alkaline metal and heavy metal chlorides may lead to increased shares of molten phases on the deposit surfaces which makes the deposits more sticky and thereby speeds up deposit growth.

The data presented in this paper and the conclusions regarding aerosol and deposit formation drawn should in the following be used as a basis for the validation of aerosol and deposit formation simulation tools and to improve the prediction correctness of these tools. Moreover, the data provide interesting information about the chemical compositions of aerosol particles in the different sections of the MSW boiler investigated in particular respectively for MSW combustion in general.

## 5. REFERENCES

- 1 VEJAHATI F., XU Z., GUPTA R., 2010: Trace elements in coal: Associations with coal and minerals and their behaviour during coal utilization – A review, in: *Fuel* 89 (2010) 904–911
- 2 SUI J., XU M., QIU J., QIAO Y., YU Y., LIU X., GAO X., 2005: Numerical Simulation of Ash Vaporization during Pulverized Coal Combustion in the Laboratory-Scale Single-Burner Furnace, *Energy & Fuels* 2005, 19, 1536-1541
- 3 JOKINIEMI, J.K., LAZARIDIS, M., LEHTINEN, K.E.J., KAUPPINEN, E.I., 1994: Numerical simulation of vapour-aerosol dynamics in combustion processes, in: *Journal of Aerosol Science*, Vol. 25, No. 3, pp. 429-446.
- 4 CHRISTENSEN K. A., 1995: The Formation of Submicron Particles from the Combustion of Straw, Ph.D. Thesis, ISBN 87-90142-04-7, Department of Chemical Engineering (ed), Technical University of Denmark, Lyngby, Denmark
- 5 JÖLLER M., BRUNNER T., OBERNBERGER I., 2007: Modelling of aerosol formation during biomass combustion for various furnace and boiler types. In: *Fuel Processing Technology*, Vol. 88, pp. 1136-1147
- 6 BRUNNER T., FRIESENBICHLER J., OBERNBERGER I., BERNER A., 2007: Development, test and application of a new low-pressure impactor for particle sampling at high temperatures up to about 1,000°C. In: *Proc of the Int. Conf. “Impacts of Fuel Quality on Power Production”*, EPRI report No. 1014551 (2007), pp.7-61 to 7-76, EPRI (Ed.), Palo Alto, CA; USA
- 7 OBERNBERGER I., 2007: Aerosol formation mechanisms, newest results. Workshop on Aerosols in Biomass Combustion, Jyväskylä, Finland, September 2007; <http://www.ieabcc.nl/> [31.05.2010]
- 8 BRUNNER T., 2006: Aerosols and coarse fly ashes in fixed-bed biomass combustion. PhD-thesis, book series “Thermal Biomass Utilization”, Volume 6, Graz University of Technology. ISBN 3-9501980-2-4